Atmospheric and Oceanic Science Letters 15 (2022) 100193

Contents lists available at ScienceDirect

Atmospheric and Oceanic Science Letters

journal homepage:
http://www.keaipublishing.com/en/journals/atmospheric-and-oceanic-science-letters/

Impacts of strong El Niño on summertime near-surface ozone over China

Mengyun Li [a], Yang Yang [a,*], Pinya Wang [a], Dongsheng Ji [b], Hong Liao [a]

[a] Jiangsu Key Laboratory of Atmospheric Environment Monitoring and Pollution Control, Jiangsu Collaborative Innovation Center of Atmospheric Environment and Equipment Technology, School of Environmental Science and Engineering, Nanjing University of Information Science and Technology, Nanjing, China
[b] State Key Laboratory of Atmospheric Boundary Layer Physics and Atmospheric Chemistry, Institute of Atmospheric Physics, Chinese Academy of Sciences, Beijing, China

ARTICLE INFO

Keywords:
El Niño
Ozone
GEOS-Chem
关键词:
厄尔尼诺
臭氧
GEOS-Chem

ABSTRACT

The influences of strong El Niño events (1997/98 and 2015/16) on summertime near-surface ozone (O_3) concentrations over China are investigated using the GEOS-Chem model. The results show that near-surface O_3 concentrations increased by a maximum of 6 ppb (parts per billion) during the summer of the developing phase of the 1997/98 El Niño in northeastern China, mainly due to the increased chemical production related to the hot and dry conditions. Besides, the O_3 concentration increased by 3 ppb during the developing summer of both the 1997/98 and 2015/16 El Niño in southern China. It was linked to the weakened prevailing monsoon winds, which led to the accumulation of O_3 in southern China. In contrast, in the summer of the decaying phase of the two El Niño events, O_3 concentrations decreased over many regions of China when the El Niño reversed to the cooling phase. This highlights that El Niño plays an important role in modulating near-surface O_3 concentrations over China.

摘要
利用全球大气化学三维模式 (GEOS-Chem) 模拟研究两次强厄尔尼诺事件 (1997/98和2015/16) 对中国夏季近地面臭氧 (O_3) 浓度的影响. 结果表明1997/98年厄尔尼诺事件发展期夏季中国东北区域O_3浓度升高, 最大值超过6ppb, 这主要归因于高温晴朗低湿等气象因素导致O_3化学生成升高. 此外, 两次厄尔尼诺事件发展期夏季O_3浓度在中国南部均增加了3ppb, 这与盛行季风减弱导致中国南方O_3局地积累有关. 相反, 在两次强厄尔尼诺衰减期夏季, 中国大部分地区O_3浓度下降伴随着海温模态转变为拉尼娜事件. 这表明厄尔尼诺在调节中国近地面O_3浓度中发挥着重要作用.

1. Introduction

Tropospheric ozone (O_3) is one of the most critical air pollutants in China (Zhao et al., 2020). It is produced by photochemical reactions through the oxidation of carbon monoxide and volatile organic compounds with the sunlight under the existence of nitrogen oxides (NO_x) (Han et al., 2011, 2020). It harms human health, damages plants and crops when close to the ground, and imposes a huge burden on economic development in China (Koken et al., 2003; Feng et al., 2015; Yang et al., 2019). Therefore, it is of great significance to understand the variations in O_3 concentrations in China and the possible influencing factors.

Meteorological parameters, i.e., atmospheric temperature, winds, and humidity, show a significant impact on regional O_3 concentrations through affecting chemical production and transport processes (Young et al., 2018). High temperatures can change O_3 concentrations by accelerating chemical production rates and natural precursor emissions (Sillman and Samson, 1995). O_3 pollution episodes occur frequently in summer with strong solar radiation. Relative humidity (RH) is also known to be an important parameter for O_3 formation, accelerating O_3 loss by reacting with hydrogen radical (Kavassalis and Murphy, 2017; Lu et al., 2018). Moreover, the existence of clouds can reduce O_3 concentrations by reducing the downward solar radiation and dampening near-surface photochemical reactions (Roy et al., 2008; Fix et al., 2018). Changes in wind fields can also influence near-surface O_3 concentrations in China through changing O_3 transport (Yang et al., 2014). Gong and Liao (2019) reported that high O_3 concentrations were accompanied by high temperatures, low RH, and downdrafts in northern China.

El Niño–Southern Oscillation (ENSO) is the strongest interannual ocean–atmosphere interaction signal of the global climate system (Jin, 1997). During its warm phase (i.e., El Niño), anomalous high sea surface temperatures (SSTs) are located over the tropical eastern Pacific Ocean, while anomalously low SST can be observed during its cold phase (i.e., La Niña) (Mosley, 2000). Two types of El Niño events have been identified based on their spatial distributions of warm SST anomalies

* Corresponding author.
E-mail address: yang.yang@nuist.edu.cn (Y. Yang).

https://doi.org/10.1016/j.aosl.2022.100193
Received 3 December 2021; Revised 31 December 2021; Accepted 10 February 2022
Available online 17 February 2022

(SSTAs): Eastern Pacific (EP) El Niño events, in which a large positive SSTA appears in the eastern Pacific; and Central Pacific (CP) El Niño events, in which a large positive SSTA is located in the equatorial central Pacific (Weng et al., 2009). Several studies have found that these two types of El Niño have different teleconnections and regional climatic effects (Yuan and Yang, 2012; Ren et al., 2018, 2019). ENSO events have substantial impacts on atmospheric circulations and weather conditions across the globe through atmospheric teleconnections, especially strong El Niño events (Feng et al., 2019). Multiple indices show that the 1997/98 and 2015/16 El Niño events are the top two strongest events in the last 70 years (Huang et al. 2016; L'Heureux et al., 2017).

During the strong El Niño event in 2015/16, weakened wind speed was observed over the North China Plain, leading to serious air pollution in eastern China (Zeng et al., 2021). Xu et al. (2007) investigated the relationship between the long-term trend of precipitation in China and El Niño. They revealed that greater precipitation was associated with El Niño episodes in southern China, but drought occurred in the Yellow River basin. Wu et al. (2010) investigated the influence of ENSO on summer temperature in northeastern China and found that it was depressed in El Niño developing years from 1950 through to the mid-1970s. However, this relationship was weakened or even opposite in the 1980s and 1990s (Zhang et al., 2008). Previous works have pointed out that El Niño can influence meteorological factors in China (e.g., Chan et al., 2005; Xue and Liu, 2008; Chen and Wu, 2017), which may further affect the spatiotemporal distribution and chemical production of O_3 (Xu et al., 2017). However, the summertime near-surface O_3 over China affected by El Niño has been insufficiently investigated.

This paper presents an analysis of the impacts of the strong El Niño events that occurred in 1997/98 and 2015/16 on summertime O_3 concentrations in China by using the global chemical transport model GEOS-Chem. We aim to understand the impacts of El Niño on summertime near-surface O_3 concentrations over China and the physical and chemical processes behind the impacts.

2. Data and methods

GEOS-Chem, a global 3D model of atmospheric chemistry, employs a fully coupled O_3–NO_x–hydrocarbon–aerosol chemical mechanism to simulate concentrations of gas-phase pollutants (Mao et al., 2013). O_3 concentrations were simulated in this study by using version 12.9.3 of GEOS-Chem (https://geos-chem.seas.harvard.edu/) with a resolution of 2° latitude by 2.5° longitude and 47 layers in the vertical direction from the surface to 0.01 hPa. The meteorological fields were derived from version 2 of the Modern-Era Retrospective Analysis for Research and Applications (MERRA-2; https://gmao.gsfc.nasa.gov/reanalysis/MERRA-2/)—the global reanalysis dataset developed by NASA's Global Modeling and Assimilation Office. Previous studies have reported that GEOS-Chem can capture well the seasonal and interannual variations of O_3 over China (e.g., Ni et al., 2018; Wang et al., 2020; Chen et al., 2021).

Simulations were performed from the year 1990 to 2020 with varying meteorological fields. In order to remove the effects of year-to-year emission changes, all monthly emissions of O_3 precursors were fixed at the year 2017 level in the simulation. Anthropogenic emissions were from the MEIC (Multi-resolution Emissions Inventory) inventory in China. The quantitative impacts on the variations in summertime O_3 in China during strong El Niño events were obtained by comparing the variables in 1997/98 and 2015/16 with the climatological means.

The Niño3.4 index was employed to characterize the phase and intensity of the ENSO condition. It was calculated as the SSTA averaged over 5°S–5°N and 170°–120°W. The El Niño events were identified when the Niño3.4 index was higher than 0.5°C and lasted for five months. The SST data were from the Hadley Centre Sea Ice and Sea Surface Temperature dataset (https://www.metoffice.gov.uk/hadobs/hadisst/data/download.html).

3. Results

3.1 Two strong El Niño events in 1997/98 and 2015/16

Fig. 1(a) shows the monthly Niño3.4 index during 1990–2020, and the spatial distributions of the SSTA during the 1997/98 and 2015/16 El Niño events are displayed in Fig. S1. Several El Niño events can be identified during this period, with two strong El Niño events occurring in 1997/98 and 2015/16, which is consistent with previous studies (Kogan and Guo, 2017; Lim et al. 2017). The monthly variations in Niño3.4 during the two strong El Niño events (1997/98 and 2015/16) are given in Fig. 1(b), covering the developing stages to the decaying stages of the two events. Both strong El Niño events exhibited a warming signal over the central–eastern tropical Pacific in the summer (June–July–August, JJA) of the developing phase of El Niño, and then they reached their mature phase in boreal winter. The Niño3.4 index then declined rapidly in the following years. In the decaying summer, the 1997/98 El Niño had already reversed to a La Niña event, while the 2015/16 El Niño changed to a weak cooling condition.

The 1997/98 El Niño was an EP type El Niño with the maximum SST increase over the tropical eastern Pacific, whereas the 2015/16 event was a combination of CP and EP El Niño with maximum warming over the central–eastern tropical Pacific. The differences in features between the two strong El Niño events may have triggered different changes in meteorological variables and thus caused different effects on near-surface O_3 concentrations in China.

3.2 Surface O_3 anomalies over China during the two strong El Niño events

The near-surface O_3 concentrations in China are much higher in summer (JJA) than in the other seasons (Gong et al., 2018). Thus, only the O_3 concentrations in JJA are presented in the following analysis. To investigate the influences of El Niño events on summertime O_3 concentrations, the reliability of GEOS-Chem in simulating the O_3 concentration was first assessed. The JJA near-surface O_3 concentrations of the model and measurements showed similar spatial distributions (Fig. S2). The spatial correlation coefficient between the observed and simulated O_3 concentrations was 0.87 in the year 2017, implying a good performance of the model, albeit with a slight overestimation of the O_3 level in China as also reported in many previous studies (e.g., Li et al., 2019; Lu et al., 2019; Dang et al., 2021).

To quantify the influences of the strong El Niño events of 1997/98 and 2015/16 on O_3 concentrations over China, the O_3 anomalies in the developing (previous) and decaying (following) summer of the two El Niño events relative to the climatological mean (1990–2020) are shown in Fig. 2. During the developing phase of the 1997/98 event, the JJA O_3 concentration increased over most of southern and northeastern China (Fig. 2(a)). The highest O_3 concentration increases were located in northeastern China (36°–44°N, 112.5°–132.5°E), exceeding 6 ppb (or 11% of the climatological mean), while increases of about 3 ppb (or 8%) occurred in southern China (20°–32°N, 97.5°–117.5°E), especially in Sichuan, Yunnan, and Guizhou provinces. Similar features were also detected in the 2015/16 event (Fig. 2(d)) in southern China, but the concentration increase was not as significant as that in the 1997/98 event. During the El Niño decaying summer, near-surface O_3 concentrations decreased in many regions of China relative to the climatological mean. The O_3 concentrations decreased over southern China in summer 1998, in which the 1997/98 El Niño reversed to a La Niña, and negative anomalies of O_3 concentrations over central China were observed in summer 2016.

In summary, during the developing phase of a strong El Niño event, the JJA O_3 concentration in China will increase, while a reduction in O_3 levels will occur during the decaying phase of El Niño in the following summer. This suggests that strong El Niño events play an important role in modulating near-surface O_3 concentrations in China.

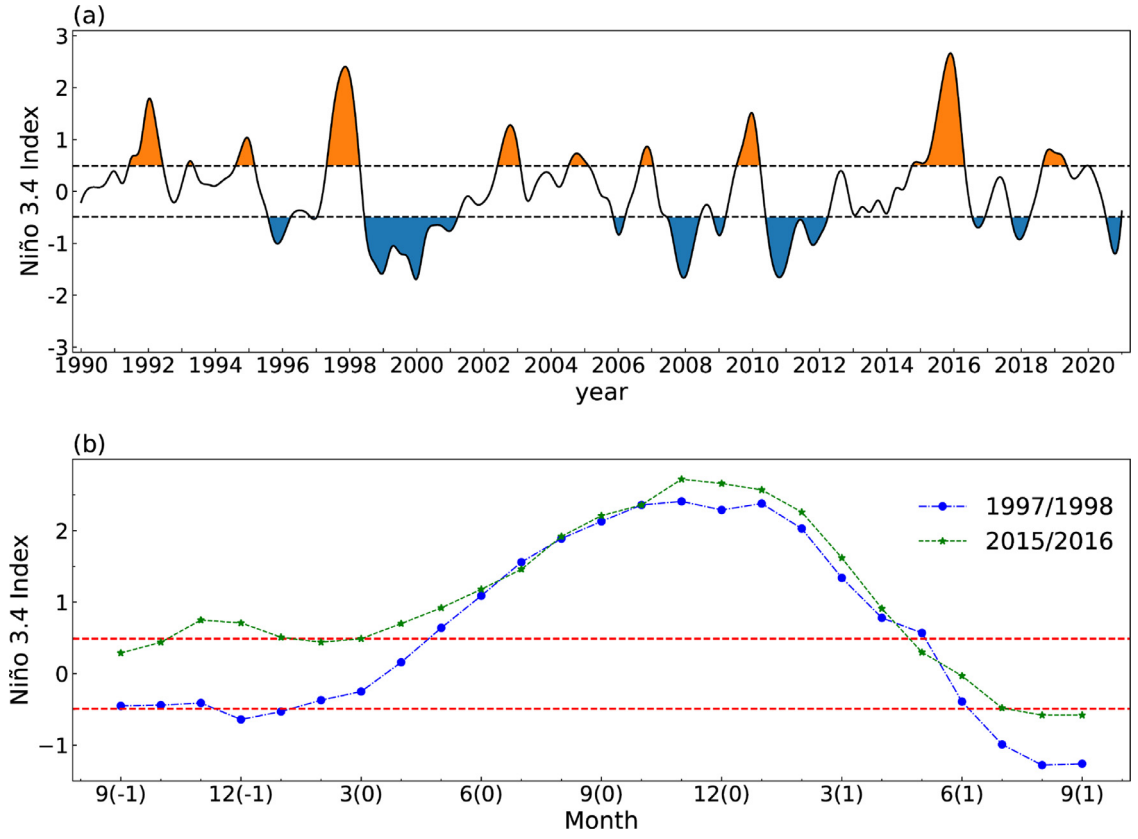

Fig. 1. (a) Monthly Niño3.4 index (units:°C) from HadISST1 during 1990–2020. The gray dotted lines denote 0.5°C and −0.5°C, respectively. Highlighted regions illustrate El Niño (orange) and La Niña (blue) events. (b) Monthly Niño3.4 index from September of the year before the El Niño year (−1) to September after the El Niño (1). The red dotted line at the top (bottom) indicates the threshold of 0.5°C (−0.5°C) for the El Niño (La Niña).

3.3 Mechanisms of El Niño impacts on O_3 in China

The results above demonstrate that O_3 concentrations over China tend to increase during the summer of the developing phase of strong El Niño events, while they tend to decrease in the following summer, which could be due to the change in the ENSO condition from El Niño to La Niña. Therefore, we only focus our discussion on the summer of the developing phase of the two El Niño events in the following analyses, and the mechanisms could also apply to the following summer when O_3 decreased in the cooling phase of ENSO. Fig. 3 shows the differences in various meteorological parameters in JJA between the two strong El Niño events and the climatological means to identify the key reasons associated with the O_3 concentration anomalies in China during the two El Niño events.

The meteorological fields in summer over China are largely influenced by the East Asian summer monsoon (EASM), with prevailing southwesterlies located over eastern China. During the summer of 1997, anomalous northeasterlies prevailed over southern China in response to the warming over the eastern Pacific (Fig. 3(a)). Likewise, in summer 2015, the EASM was weakened, featuring anomalous northerly winds in China (Fig. 3(g)). The poor dissipation conditions associated with weakened winds resulted in an accumulation of O_3 over southern China.

This hypothesis is further confirmed by the analysis of O_3 mass flux over southern China shown in Table 1. In general, 9.2 and 11.4 Tg of O_3 is imported from the west and south of southern China, respectively, while 9.6 and 8.8 Tg is exported from the east and north of southern China, from the surface to 500 hPa, related to the prevailing southwesterlies. During the two strong El Niño events, the export of O_3 from the north was reduced by 7.8 and 8.8 Tg in JJA of 1997 and 2015, respectively, relative to the climatological mean, indicating that the weakened southerlies were the main reason for the increase in O_3 concentration over southern China during the El Niño events. More O_3 imported from the west (by 2.7 and 2.8 Tg in 1997 and 2015, respectively) also contributed to the increase in O_3. Changes in vertical mass flux also perturbed the O_3 budget, by −1.1 Tg in 1997 and 0.88 Tg in 2015 compared to the normal condition, but the changes were smaller than the horizontal mass fluxes. During the summer of the developing phase of El Niño, negative temperature anomalies occurred in southern China, which were not favorable for the chemical production of O_3.

An anomalous high at 500 hPa was located in northeastern China in the summer of 1997, with increases in air temperature and downwelling shortwave radiation and decreases in RH (Fig. 3). The hot and dry weather conditions were favorable for the chemical production of O_3. As a result, the O_3 concentration increased in the summer of 1997 over northeastern China. However, unlike in 1997, an anomalous low was located in northeastern China and the North China Plain, leading to

Table 1 The horizontal and vertical mass fluxes (Tg) of JJA O_3 concentration from the surface to 500 hPa over southern China (20°–32°N, 97.5°–117.5°E) in 1997 and 2015, along with the climatological mean, as well as the changes in mass fluxes in 1997 and 2015 relative to the climatological mean. Positive values indicate incoming fluxes and negative values indicate outgoing fluxes. The climatological mean values are the averages over 1990–2020.

	1997	2015	Mean	1997 minus mean	2015 minus mean
Horizontal mass flux					
East	−11.97	−18.12	−9.62	−2.35	−8.50
West	11.87	11.97	9.21	2.66	2.76
North	−1.02	−0.03	−8.84	7.82	8.81
South	9.38	11.24	11.39	−2.01	−0.15
Vertical mass flux					
Top	5.11	7.09	6.21	−1.10	0.88

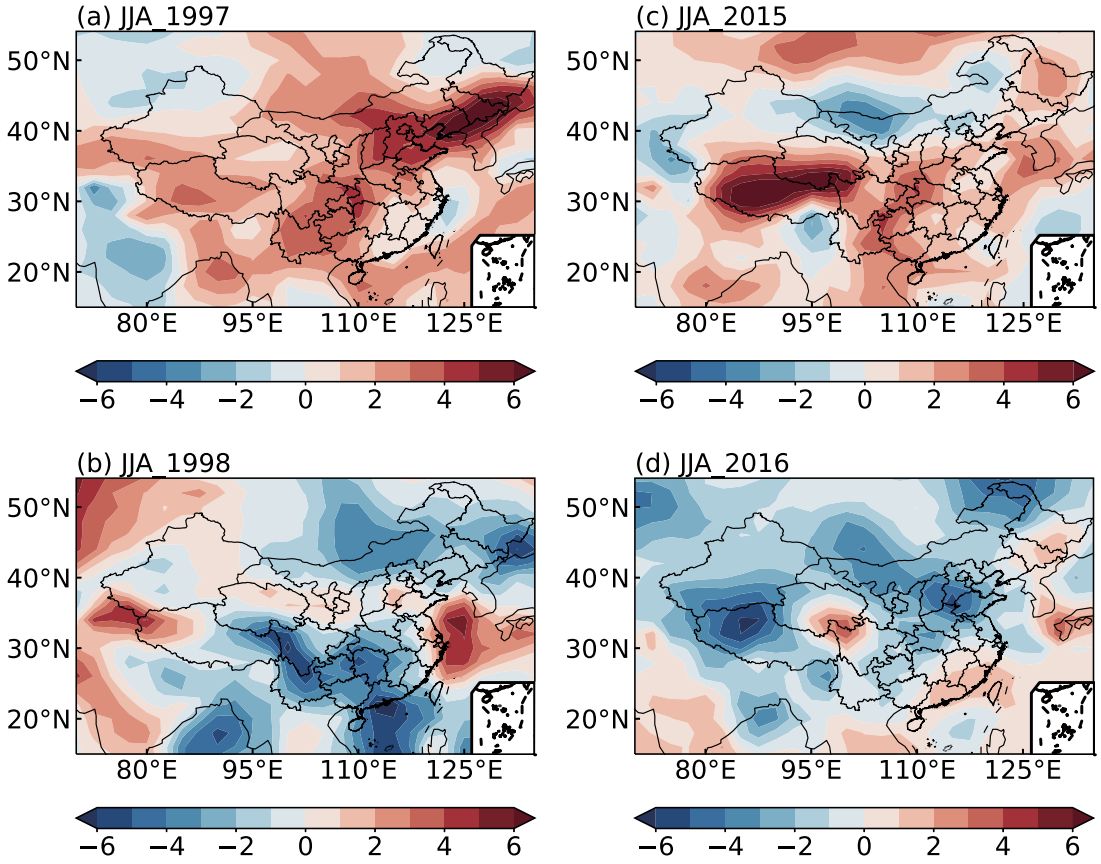

Fig. 2. Spatial distribution of JJA O_3 concentration anomalies (units: ppb) during the (a, c) developing phase and (b, d) decaying phase of the 1997/98 and 2015/16 EI Niño event, respectively, relative to the climatological mean (1990–2020).

a decrease in temperature and increase in RH, which was not conducive to O_3 production. Therefore, through the combination of chemical and physical processes, there was no obvious change in O_3 concentration in northeastern China in JJA 2015.

To summarize, the increases in O_3 concentrations over southern China during the developing summer of the two strong El Niño were due to the accumulation of O_3 driven by physical processes, especially horizontal advection. However, chemical production of O_3 was the primary reason for the increase in JJA O_3 levels over northeastern China. The different patterns of the two strong El Niño events were likely due to the different El Niño types, i.e., with 1997/98 being a typical EP type event and 2015/16 a combination of CP and EP type events.

4. Summary and discussion

In this study, the impacts of two strong El Niño events, i.e., 1997/98 and 2015/16, on summertime near-surface O_3 concentrations over China were quantitatively examined based on chemical transport model simulations. During the summer of the developing phase of El Niño, near-surface O_3 concentrations increased in China, but they decreased during the following decaying summer of the El Niño events, which was related to the transition of ENSO conditions from El Niño to La Niña causing opposite O_3 changes. In summer 1997, near-surface O_3 anomalies increased by a maximum of 6 ppb (11%) over northeastern China, which resulted from the enhanced chemical production of O_3 related to the hot and dry weather conditions. Increases in O_3 concentrations by 3 ppb (8%) were observed in southern China, where Sichuan, Yunnan, and Guizhou provinces had the largest positive anomalies during the developing summer of the two strong El Niño events. This was due to the accumulation of O_3 under the poor dissipation conditions linked to the weakened prevailing southerly winds. Considering the important role played by strong El Niño in modulating near-surface O_3 concentrations, the variations in ENSO conditions should be taken into account in future air pollution prediction and control.

There are some deficiencies and uncertainties in this study that could be improved upon in future research. For instance, although both strong El Niño cases showed that O_3 concentrations increased in the developing summer and decreased in the following decaying summer over China, it is difficult, based only on two events, to conclude whether this is a common feature for El Niño. Therefore, longer modeling and observational data covering more strong El Niño events are needed to explore the O_3 responses and mechanisms. In the following summer of the two strong El Niño events, negative O_3 concentration anomalies occurred in some regions of China, accompanied by La Niña events. Whether La Niña events play any role in determining the O_3 concentration over China and what the differences are between El Niño and La Niña needs further investigation. In addition, this study was based on model simulations, and more observational data to assess the performance of the model are needed. Meanwhile, the anthropogenic emissions of O_3 precursor gases that differed in magnitude were fixed at their levels in 2017, which may have caused a small bias in the calculation of the O_3 influenced by these El Niño events. And finally, the changes in meteorological parameters during the El Niño events may also have been influenced by other climate signals, which can be examined in future with climate model simulations in which SST alone is perturbed.

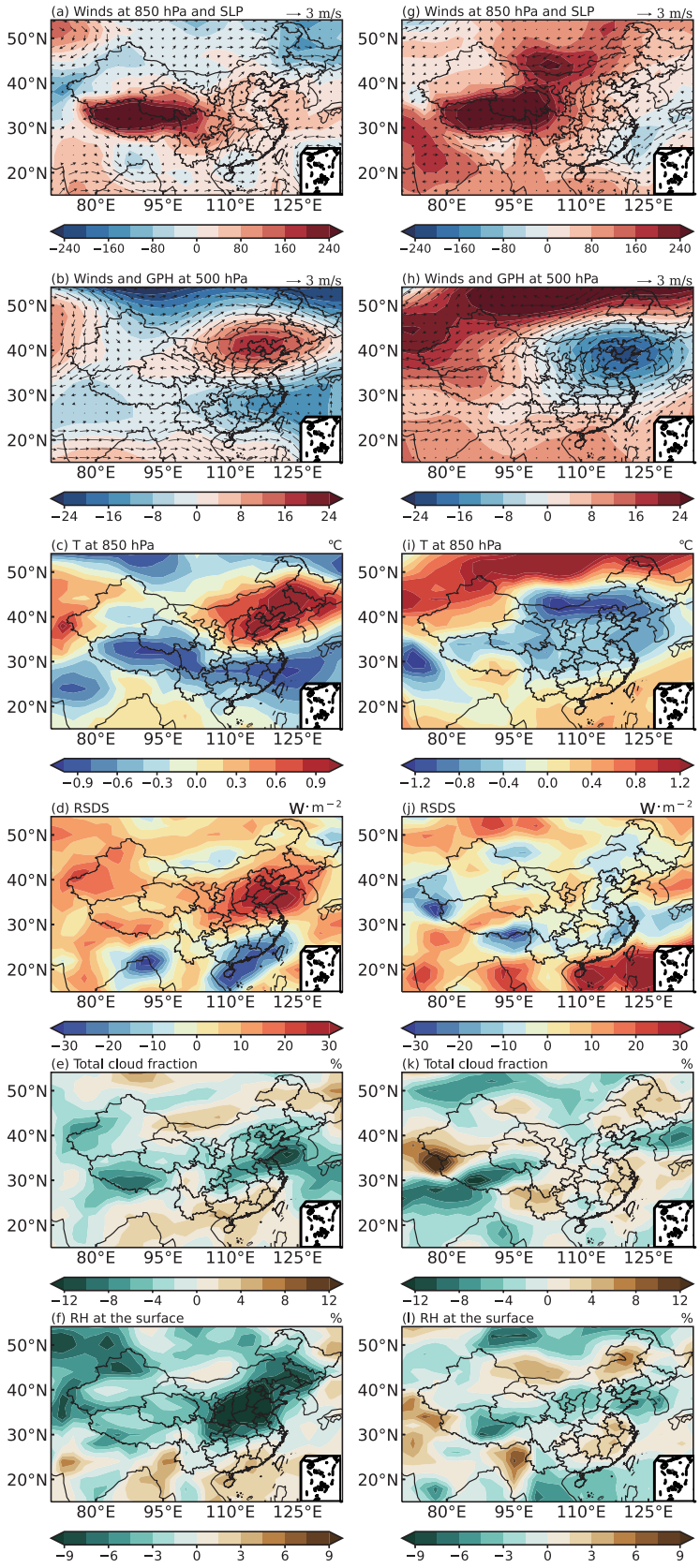

Fig. 3. Anomalies of JJA mean (a, g) 850 hPa winds (vectors; units: m s^{-1}) and sea level pressure (SLP; contours; units: Pa), (b, h) 500 hPa winds (vectors; units: m s^{-1}) and geopotential height (GPH; contours; units: m), (c, i) 850 hPa air temperature (*T*; units:°C), (d, j) downwelling shortwave radiation at the surface (RSDS; units: W m^{-2}), (e, k) total cloud fraction (%), and (f, l) RH (%) at the surface, in 1997 and 2015, respectively, relative to the climatological mean (1990–2020), derived from MERRA-2 reanalysis data.

Funding

This study was supported by the National Key Research and Development Program of China [grant numbers 2020YFA0607803 and 2019YFA0606800] and the National Natural Science Foundation of China [grant number 41975159].

Supplementary materials

Supplementary material associated with this article can be found, in the online version, at doi:10.1016/j.aosl.2022.100193.

References

Chan, J.C.L., Zhou, W., 2005. PDO, ENSO and the early summer monsoon rainfall over south China. Geophys. Res. Lett. 32 (8), L08810.
Chen, S., Wu, R., 2017. Interdecadal changes in the relationship between interannual variations of spring North Atlantic SST and Eurasian surface air temperature. J. Clim. 30 (10), 3771–3787.
Chen, X., Jiang, Z., Shen, Y., Li, R., Fu, Y., Liu, J., Han, H., et al., 2021. Chinese regulations are working—why is surface ozone over industrialized areas still high? Applying lessons from northeast US air quality evolution. Geophys. Res. Lett. 48 (14), e2021GL092816.
Dang, R., Liao, H., Fu, Y., 2021. Quantifying the anthropogenic and meteorological influences on summertime surface ozone in China over 2012–2017. Sci. Total Environ. 754, 142394.
Feng, J., Li, J., Liao, H., Zhu, J., 2019. Simulated coordinated impacts of the previous autumn North Atlantic Oscillation (NAO) and winter El Niño on winter aerosol concentrations over eastern China. Atmos. Chem. Phys. 19 (16), 10787–10800.
Feng, Z., Hu, E., Wang, X., Jiang, L., Liu, X., 2015. Ground-level O_3 pollution and its impacts on food crops in China: a review. Environ. Pollut. 199, 42–48.
Fix, M.J., Cooley, D., Hodzic, A., Gilleland, E., Russell, B.T., Porter, W.C., Pfister, G.G., 2018. Observed and predicted sensitivities of extreme surface ozone to meteorological drivers in three US cities. Atmos. Environ. 176, 292–300.
Gong, C., Liao, H., 2019. A typical weather pattern for ozone pollution events in North China. Atmos. Chem. Phys. 19 (22), 13725–13740.
Gong, X., Hong, S., Jaffe, D.A., 2018. Ozone in China: Spatial distribution and leading meteorological factors controlling O_3 in 16 Chinese cities. Aerosol Air Qual. Res. 18 (9), 2287–2300.
Han, S., Bian, H., Feng, Y., Liu, A., Li, X., Zeng, F., Zhang, X., 2011. Analysis of the relationship between O_3, NO and NO_2 in Tianjin, China. Aerosol Air Qual. Res. 11 (2), 128–139.
Han, S., Yao, Q., Tie, X., Zhang, Y., Zhang, M., Li, P., Cai, Z., 2020. Analysis of surface and vertical measurements of O_3 and its chemical production in the NCP region, China. Atmos. Environ. 241, 117759.
Huang, B., L'Heureux, M., Hu, Z.Z., Zhang, H.M., 2016. Ranking the strongest ENSO events while incorporating SST uncertainty. Geophys. Res. Lett. 43 (17), 9165–9172.
Jin, F.F., 1997. An equatorial ocean recharge paradigm for ENSO. Part I: conceptual model. J. Atmos. Sci. 54 (7), 811–829.
Kavassalis, S.C., Murphy, J.G., 2017. Understanding ozone-meteorology correlations: A role for dry deposition. Geophys. Res. Lett. 44 (6), 2922–2931.
Kogan, F., Guo, W., 2017. Strong 2015–2016 El Niño and implication to global ecosystems from space data. Int. J. Remote Sens. 38 (1), 161–178.
Koken, P.J., Piver, W.T., Ye, F., Elixhauser, A., Olsen, L.M., Portier, C.J., 2003. Temperature, air pollution, and hospitalization for cardiovascular diseases among elderly people in Denver. Environ. Health Perspect. 111 (10), 1312–1317.
L'Heureux, M.L., Takahashi, K., Watkins, A.B., Barnston, A.G., Becker, E.J., Di Liberto, T.E., Gamble, F., et al., 2017. Observing and predicting the 2015/16 El Niño. Bull. Amer. Meteorol. Soc. 98 (7), 1363–1382.
Li, K., Jacob, D.J., Liao, H., Shen, L., Zhang, Q., Bates, K.H., 2019. Anthropogenic drivers of 2013-2017 trends in summer surface ozone in China. Proc. Nat. Acad. Sci. U.S.A. 116 (2), 422–427.
Lim, Y.K., Kovach, R.M., Pawson, S., Vernieres, G., 2017. The 2015/16 El Niño event in context of the MERRA-2 reanalysis: a comparison of the tropical Pacific with 1982/83 and 1997/98. J. Clim. 30 (13), 4819–4842.
Lu, X., Hong, J., Zhang, L., Cooper, O.R., Schultz, M.G., Xu, X., Wang, T., Gao, M., Zhao, Y., Zhang, Y., et al., 2018. Severe surface ozone pollution in China: a global perspective. Environ. Sci. Technol. Lett. 5 (8), 487–494.
Lu, X., Zhang, L., Chen, Y., Zhou, M., Zheng, B., Li, K., Liu, Y., Lin, J, Fu, T., Zhang, Q., 2019. Exploring 2016–2017 surface ozone pollution over China: source contributions and meteorological influences. Atmos. Chem. Phys. 19 (12), 8339–8361.
Mao, J., Paulot, F., Jacob, D.J., Cohen, R.C., Crounse, J.D., Wennberg, P.O., Keller, C.A., Hudman, R.C., Barkley, M.P., Horowitz, L.W., 2013. Ozone and organic nitrates over the eastern United States: sensitivity to isoprene chemistry. J. Geophys. Res. 118 (19), 11256–11268.
Mosley, M.P., 2000. Regional differences in the effects of El Niño and La Niña on low flows and floods. Hydrol. Sci. J. 45 (2), 249–267.
Ni, R., Lin, J., Yan, Y., Lin, W., 2018. Foreign and domestic contributions to springtime ozone over China. Atmos. Chem. Phys. 18 (15), 11447–11469.
Ren, H.L., Lu, B., Wan, J., Tian, B., Zhang, P., 2018. Identification standard for ENSO events and its application to climate monitoring and prediction in China. J. Meteorol. Res. 32 (6), 923–936.
Ren, H.L., Scaife, A.A., Dunstone, N., Tian, B., Liu, Y., Ineson, S., Lee, J., et al., 2019. Seasonal predictability of winter ENSO types in operational dynamical model predictions. Clim. Dyn. 52 (7), 3869–3890.
Roy, S., Beig, G., Jacob, D., 2008. Seasonal distribution of ozone and its precursors over the tropical Indian region using regional chemistry-transport model. J. Geophys. Res. 113 (D21), D21307.
Sillman, S., Samson, P.J., 1995. Impact of temperature on oxidant photochemistry in urban, polluted rural and remote environments. J. Geophys. Res. 100 (D6), 11497–11508.
Wang, X., Jacob, D.J., Fu, X., Wang, T., Breton, M.L., Hallquist„ M., Liu, Z., MeDuffie, E.E., Liao, H., 2020. Effects of anthropogenic chlorine on $PM_{2.5}$ and ozone air quality in China. Environ. Sci. Technol. 54 (16), 9908–9916.
Weng, H., Behera, S.K., Yamagata, T., 2009. Anomalous winter climate conditions in the Pacific rim during recent El Niño Modoki and El Niño events. Clim. Dyn. 32 (5), 663–674.
Wu, R., Yang, S., Liu, S., Sun, L., Lian, Y., Gao, Z., 2010. Changes in the relationship between Northeast China summer temperature and ENSO. J. Geophys. Res. 115 (D21), D21107.
Xu, L., Yu, J.Y., Schnell, J.L., Prather, M.J., 2017. The seasonality and geographic dependence of ENSO impacts on US surface ozone variability. Geophys. Res. Lett. 44 (7), 3420–3428.
Xu, Z.X., Li, J.Y., Takeuchi, K., Ishidaira, H., 2007. Long-term trend of precipitation in China and its association with the El Niño–southern oscillation. Hydrol. Processes 21 (1), 61–71.
Xue, F., Liu, C.Z., 2008. The influence of moderate ENSO on summer rainfall in eastern China and its comparison with strong ENSO. Chin. Sci. Bull. 53 (5), 791–800.
Yang, P., Zhang, Y., Wang, K., Doraiswamy, P., Cho, S.H., 2019. Health impacts and cost-benefit analyses of surface O_3 and $PM_{2.5}$ over the US under future climate and emission scenarios. Environ. Res. 178, 108687.
Yang, Y., Liao, H., Li, J., 2014. Impacts of the East Asian summer monsoon on interannual variations of summertime surface-layer ozone concentrations over China. Atmos. Chem. Phys. 14 (13), 6867–6879.
Young, P.J, Naik, V., Fiore, A.M., Gaudel, A., Guo, J., Lin, M.Y., Neu, J.L., et al., 2018. Tropospheric Ozone Assessment Report: Assessment of global-scale model performance for global and regional ozone distributions, variability, and trends. Elem. Sci. Anth. 6, 10.
Yuan, Y., Yang, S., 2012. Impacts of different types of El Niño on the East Asian climate: Focus on ENSO cycles. J. Clim. 25 (21), 7702–7722.
Zeng, L., Yang, Y., Wang, H., Wang, J., Li, J., Ren, L., Li, H., Zhou, Y., Wang, P., Liao, H., 2021. Intensified modulation of winter aerosol pollution in China by El Niño with short duration. Atmos. Chem. Phys. 21 (13), 10745–10761.
Zhang, T., Zhu, J., Yang, X., Zhang, X, et al., 2008. Correlation changes between rice yields in North and Northwest China and ENSO from 1960 to 2004. Agric. For. Meteorol. 148 (6–7), 1021–1033.
Zhao, S., Yin, D., Yu, Y., Kang, S., Qin, D., Dong, L., 2020. $PM_{2.5}$ and O_3 pollution during 2015–2019 over 367 Chinese cities: spatiotemporal variations, meteorological and topographical impacts. Environ. Pollut. 264, 114694.